

Effect of turbulent fluctuations on the behaviour of fountains in stratified environments

This article has been downloaded from IOPscience. Please scroll down to see the full text article.

2010 J. Phys.: Conf. Ser. 246 012015

(<http://iopscience.iop.org/1742-6596/246/1/012015>)

View [the table of contents for this issue](#), or go to the [journal homepage](#) for more

Download details:

IP Address: 164.73.83.34

The article was downloaded on 21/03/2011 at 12:24

Please note that [terms and conditions apply](#).

Effect of turbulent fluctuations on the behaviour of fountains in stratified environments

D Freire¹, C Cabeza¹, S Pauletti¹, G Sarasúa¹, I Bove¹, G Usera², Arturo C Martí¹

¹Instituto de Física, Universidad de la República, Igua 4225, 11400 Montevideo, Uruguay

²Instituto de Mecánica de los Fluidos, Facultad de Ingeniería, Universidad de la República, CC 30, 11000 Montevideo, Uruguay

E-mail: marti@fisica.edu.uy

Abstract. The interaction between a turbulent fountain and its stratified environment was studied. A heavy fluid, cold water, was injected vertically upwards into a linearly stratified medium. The round heavy-fluid jet reaches a maximum height before it begins to fall due to the effect of gravity. Because of the effects of friction and mixing, the vertical momentum and density of the jet fluid decrease as it submerges to an intermediate height of zero buoyancy. At this point, the jet fluid spreads as a horizontal front, intruding into the stratified environment. The degree of fluctuation in the proximity of the injection point was studied under both unrestricted- and restricted-flow configurations at the injection, using two differently sized stainless-steel woven-wire screens at the injection port as flow-restricting means. Using visualization and velocimetry techniques, both maximum and spreading heights were found to decrease with increasing turbulence at the point of injection.

1. Introduction

Frosts significantly impact agriculture and food production worldwide. Broadly, frosts may be classified as either advection or radiation frosts. Advection frosts result from the passage of a cold, dry polar air mass over a delimited area. Although these frosts have devastating effects, they are extremely infrequent in temperate regions. In contrast, radiation freezing occurs in temperate regions—on clear, still winter or spring nights—tens of times yearly. A high frequency of radiation frosts results in considerable economic losses due to crop failure, the late spring frosts being especially harmful. The damage resulting from freezing depends on both exposure time and temperature. Temperatures below a sharp limit result in severe crop damage, with nearly all the vegetable tissues of temperate crops being virtually damaged within a couple of hours at $-2\text{ }^{\circ}\text{C}$ [1].

Under radiation frost conditions, the Earth's surface cools by radiation through the atmosphere, which is semitransparent to long-wavelength electromagnetic radiation. Once the surface temperature has decreased below that of the surrounding air, the latter cools down by radiation and, to a lesser extent, by turbulent convection and molecular conduction. The lower layers of atmospheric air — within a few tens of meters of the ground— are subject to cooling at a rate decreasing with altitude. Under these conditions, air temperature increases with altitude through the lower atmospheric layers. Moreover, the stratified structure of lower atmospheric air is stabilized as the lowest layers are the coldest and therefore the densest ones. In this situation, referred to as temperature inversion, the atmosphere can be ideally represented as a vertical succession of strata —*i.e.* horizontal layers of atmospheric air— of increasing density with increasing proximity to the Earth's surface.

Several strategies, such as the installation of heaters, sprinklers, and even the use of helicopters, may be adopted to reduce damages resulting from radiation frosts; yet, all these solutions have serious drawbacks. Another commercially available alternative, the Selective Inverted Sink (SIS) [2] operates by selective withdrawal of the densest (coldest) air layer. This device ejects cold air upward through a source nozzle, supplying the required mechanical power. The cold-air jet not only expels (air from the earth's surface) but also entrains and suctions fluid from the horizontal layers it runs through. It is estimated that the volumetric flow-rate of the jet doubles every three orifice diameters away from the nozzle [3].

Although the usefulness of the SIS may come as a surprise, its suitability for the mitigation of radiation frosts has been advocated [1,2]. With a view to contributing to the improvement of SIS design, a laboratory model was here studied. A relationship was established between the maximum height reached by an upward jet of cold air in a temperature-stratified medium and the turbulence structure of the jet stream.

Turbulent fountains. A fountain is usually defined as a jet in which the buoyancy force acts —as a result of the temperature difference between the jet fluid and the environmental fluid— in the opposite direction to that of the jet velocity. In view of the multiple applications of light-fluid jets — *i.e.* where the density of the jet fluid, at ground level, is lower than that of the environmental fluid—, they have been more widely studied than heavy-fluid jets. However, several important applications of the latter include selective withdrawal, desalination plants, and the replenishment of magma chambers [4-9]. The here-studied SIS model also constitutes an example of heavy-fluid jets.

The upward ejection of dense fluid through a nozzle placed at the base of a tank produces the desired fountain [5-7]. The fluid inside the container has a stable stratification and a density lower than or equal to that of the jet fluid. The jet entrains the environmental fluid into the initial upflow, and the fountain radius increases as the jet fluid density decreases with height. The momentum of the rising fluid decreases as a result of the opposing buoyancy force until it comes to a halt at an initial height. The downflow forming at the upper end of the fountain reduces the fountain height to a final value — on account of turbulent interaction with the upflow— and mixes with the environmental fluid.

In a homogeneous environment, the falling fluid always remains denser than the environment, and the flow spreads across the base of the tank. However, in a stratified medium the final density of the downflow depends strongly on the strength of the environment stratification. Any entrainment of environmental fluid from intermediate strata reduces the density of the downflow to equal that of the environment at some point at an intermediate height. At this point, the downward flow still has some momentum, so a small overshoot is formed before it finally intrudes into the environment. The

thickness of the resulting outflow is comparable to the spreading height near the fountain axis but quickly decreases with increasing radial distance.

Whenever a jet fluid has negative buoyancy at the base of a tank containing a stably stratified fluid, the behaviour of the fountain flow lies between that of homogeneous and stratified media. In this work, experimental results describe the dependence of the jet evolution on the turbulence level at the point of injection. A description of the jet flow obtained by PIV is also provided.

2. Experimental setup and visualization techniques

The experimental setup shown in Fig. 1, comprises a prismatic container whose lateral walls consist of 1.5 cm-thick acrylic panes of 40 cm in width and 100 cm in height. The bottom and top walls consist of thermostated aluminium plates of 1.0 cm in thickness.

In order to ensure a constant inlet flow, feed water was discharged from an elevated tank, keeping the feed water level constant by means of an overflow system (Fig. 1, top left). Feed water, running by gravity through a pipe from the feed tank to the inlet port, was injected through a nozzle located at the container bottom. The water flow-rate at the inlet was measured (McMillan 101-8 flow meter) and controlled by means of a valve. The container was initially full of water. A vent was fitted in the top wall to allow the outflow of excess water from the container.

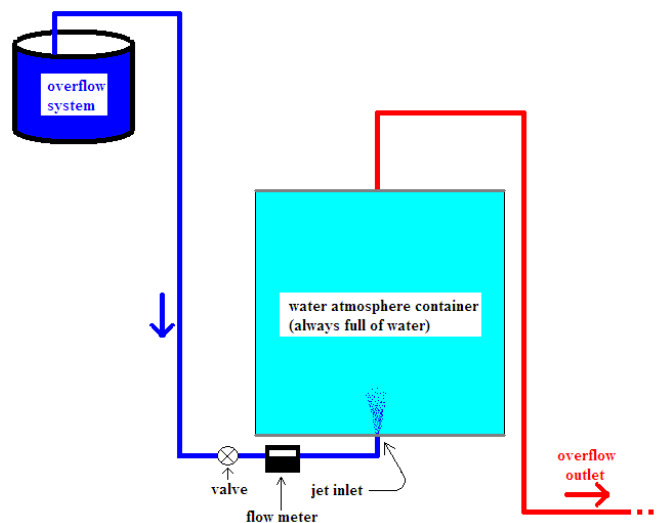


Figure 1: Experimental setup

The fluid within the container consisted of linearly stratified water at 15 °C at the base and 40 °C at the top. In order to obtain such stratification, different intermediate water layers were carefully heated by means of a sliding resistance. Various thermocouples were used to monitor the temperature of different water layers.

The density profile of the resulting stratified medium was allowed sufficient time (*c.a.* 2 h) to stabilize. The temperatures of the top and bottom walls were kept constant (by means of electrical resistance and external cooling water circuit). The lateral walls of the container were insulated with 10.0-cm deep panes of expanded polystyrene. Work conditions at the start of the run and the respective uncertainty values are shown in Fig. 2. The medium stratification fitted a linear model.

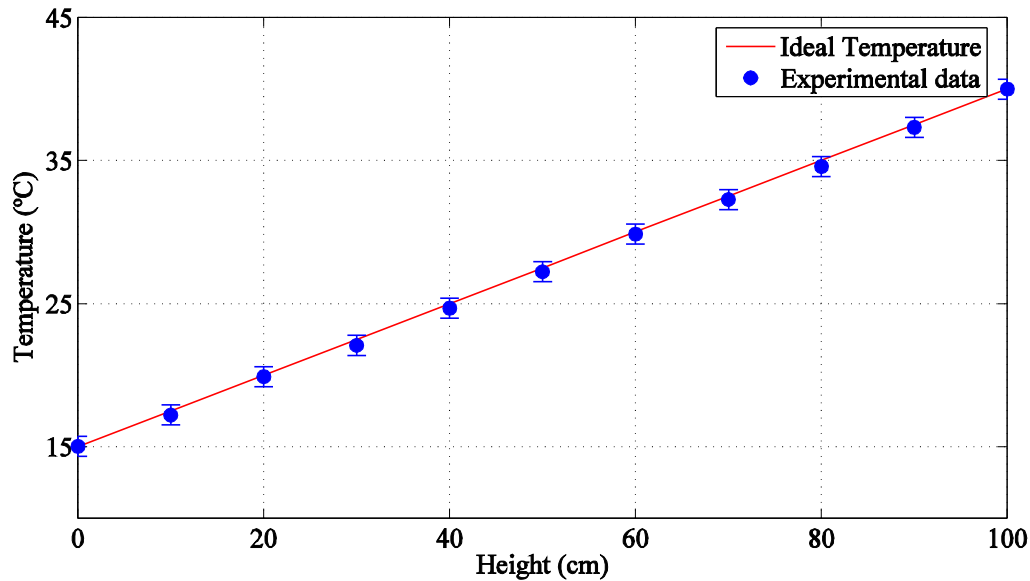


Figure 2: Characterization of the stratified environment

Jet water at 15 °C was injected through an inlet port of 8.0 mm diameter located in the centre of the base wall. Different degrees of turbulence were generated by means of a set of stainless-steel woven-wire mesh screens placed at the inlet port. Three situations have been studied: a) unrestricted flow at injection point; b) restricted flow at injection point by means of 40-mesh screen with wire diameter of 0.22 mm; and c) 80-mesh screen with wire diameter of 0.18 mm. The flow rate was kept at 0.30 L.min⁻¹ during all runs.

Digital Particle Image Velocimetry (DPIV) was used to determine the velocity field and characterize the turbulence intensity, by application over a small area immediately above the point of injection. Both the environmental and the jetted fluid were appropriately seeded with 50 µm diameter polyamide particles. The fluid was illuminated by means of a 500 mW green laser sheet of 2.0 mm in thickness. Images were captured by a PULNIX (TMC-6740GE) camera at 500 fps and processed in MatLab using a standard algorithm.

A dying technique was used in order to analyze the overall motion of the fluid, and to visualize its intrusion into the stratified medium, as well as measure the height at which the fluid starts to spread laterally (point of zero buoyancy) after reaching its maximum altitude. The images were captured under uniform illumination by means of a PIXELINK (PL-A741) camera.

3. Turbulence generation

Once the jet passes through the different mesh screens, the flow develops appreciable disorder. In order to study these fluctuations, several images were taken within a small region in close proximity to the point of injection. Images of the jet flow were taken along the length of its axis, starting a couple of centimetres from the injection point. A plot of mean vertical velocity profiles at different heights is shown in Figure 3 for the three studied configurations. Mean velocity was determined over 4-second intervals.

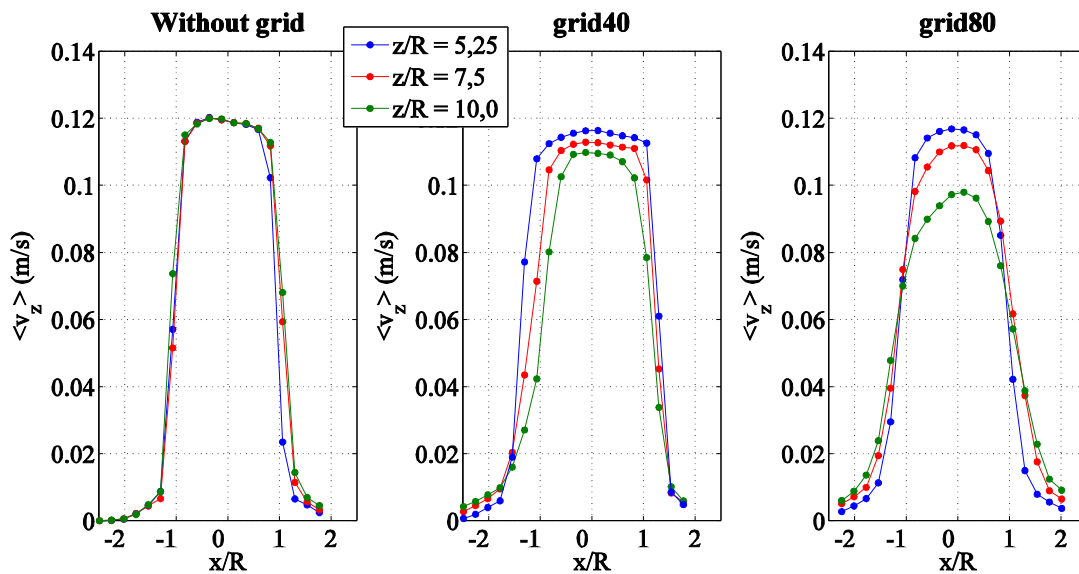


Figure 3: Mean vertical velocity profiles at different heights as a function of non-dimensional radial position under three different configurations

Standard deviations of the velocity field (σ) were calculated in order to analyze the velocity fluctuation (μ). In Figure 4, a plot of the vertical component of the velocity fluctuation (μ_z) is shown at point $z/R = 5.7$ and $x/R = 0.12$ for the three configurations. A quantitative difference was observed in the fluctuation pattern of the 40-mesh and 80-mesh screen configurations. However, no significant differences were found between the unrestricted flow and 40-mesh configurations.

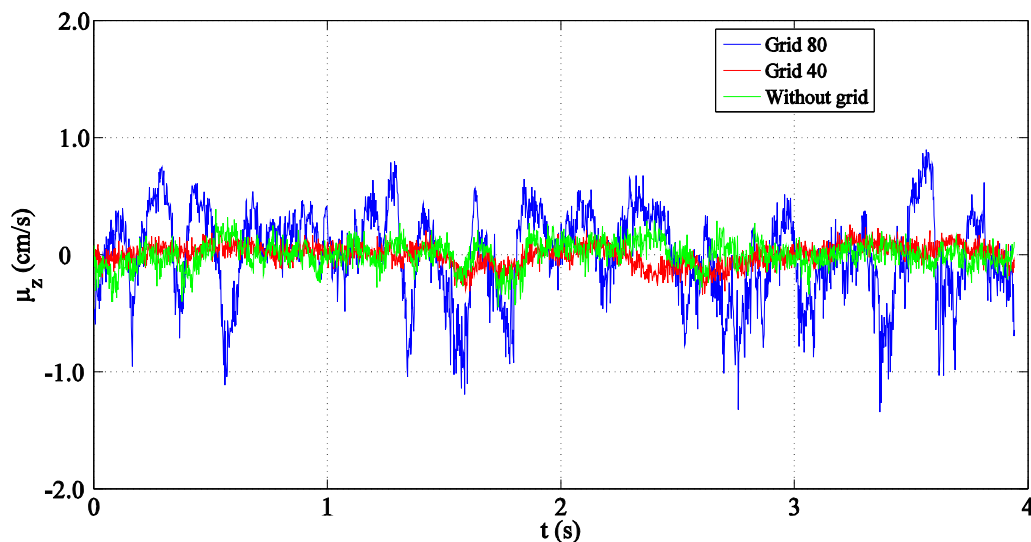


Figure 4: Fluctuation of the vertical component of the velocity (μ_z) at point $z/R = 5.7$ and $x/R = 0.12$ as function of time under three flow configurations at the jet source

A colour map of the standard deviation of the vertical component of the velocity σ_z over the capture region is shown in Fig. 5 for the three configurations studied. Asymmetries in the boundaries between the jet and the environment may be ascribed to imperfections in the mesh screen or to external

fluctuations in the pipes upstream of the inlet. Such asymmetries, appearing as a result of the transition from laminar to turbulent flow, led to different fluctuation patterns in repeated runs.

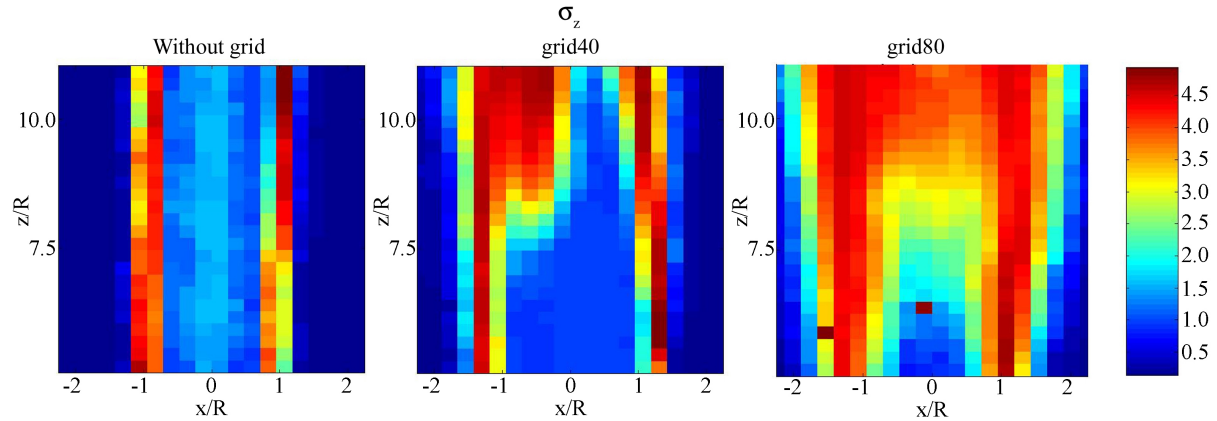


Figure 5: Standard deviation of the vertical velocity component σ_z under the different flow configurations at the injection point

Figure 6 shows the standard deviation σ_z of the vertical velocity component σ_z at different heights at the horizontal position $x/R = 1.2$. The standard deviation increased with height under the 40-mesh and 80-mesh configurations, and was consistently the greatest for the 80-mesh configuration. Using the 40-mesh configuration, fluctuations were within a range close to the range of fluctuations obtained under unrestricted flow at the injection point. Using unrestricted flow, the standard deviation of the velocity was, in good approximation, nearly constant.

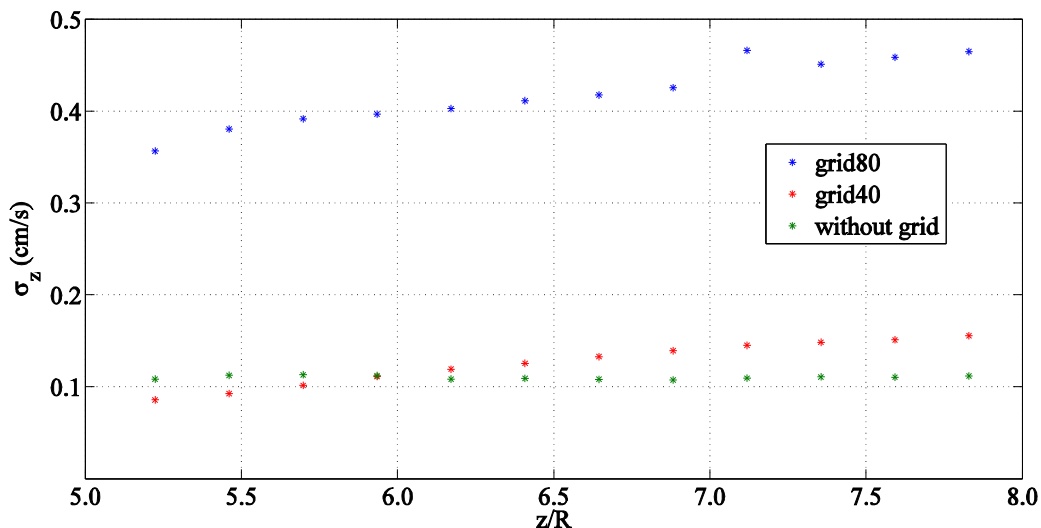


Figure 6: Standard deviation of v_z as function of the non-dimensional height z/R at $x/R = 0.12$

4. Characterization of the jet in the stratified medium

The evolution of a turbulent jet —dyed with $KMnO_4$ — injected into a stratified medium was studied for the unrestricted-flow and the 80-mesh restricted-flow configuration.

Images of the entire container volume were taken by means of a CCD camera at 4 fps under bright, uniform illumination. Four different stages of the jet development are shown in Figure 7. Initially, the jet intruded into the stratified environment (Figure 7a) and became less dense as it warmed. It continued to rise until it reached its maximum height (Figure 7b), whence it submerged to an intermediate height at which its density (temperature) equalled that of the environment (Figure 7c), before finally spreading laterally (Figure 7d).

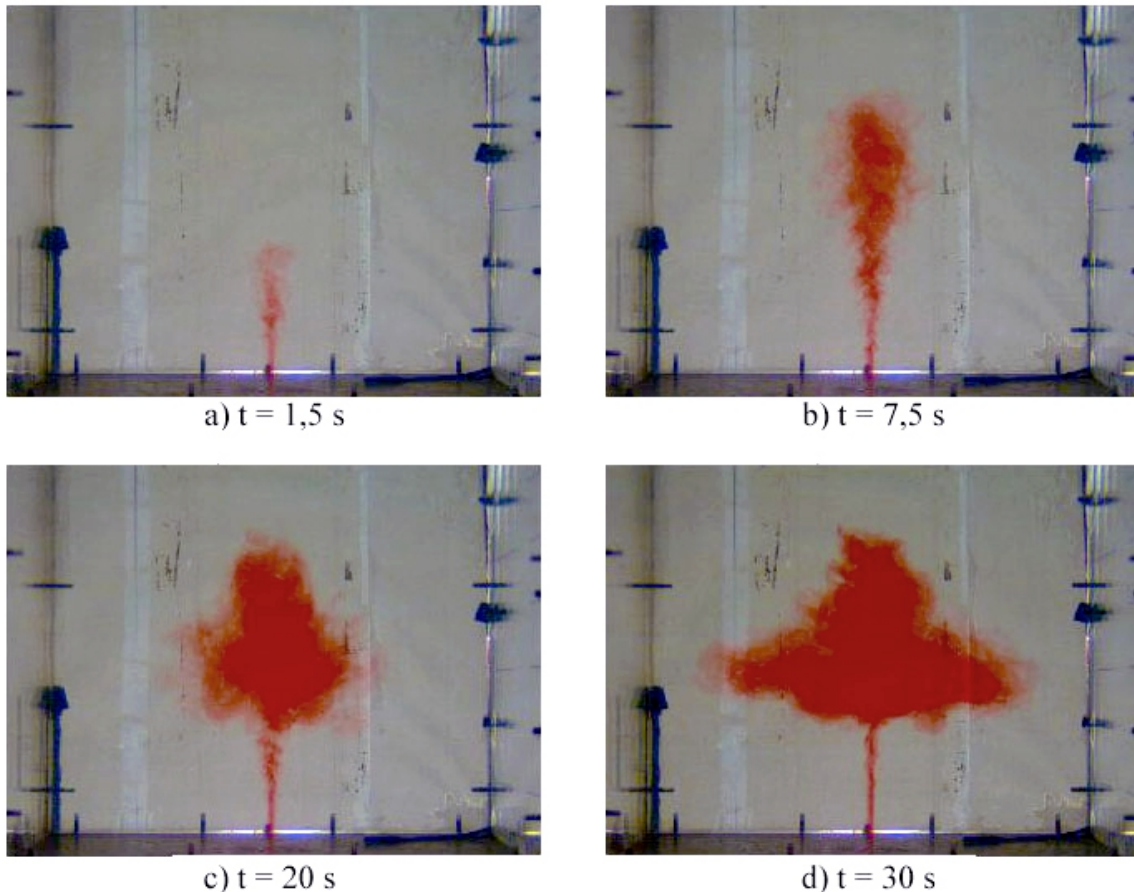


Figure 7: Jet evolution a) upon injection; b) at near-maximum height; c) in downward flow; d) spreading laterally at an intermediate zero-buoyancy height

Figure 8 shows the maximum height reached by the jet as a function of time for the unrestricted flow and 80-mesh configurations. Despite the similar behaviour of the two configurations, lower maximum height values were reached in the latter case. The intermediate height at which the downward flow intrudes into the environment was also studied. The evolution of the spreading height as function of time is shown in Figure 9.

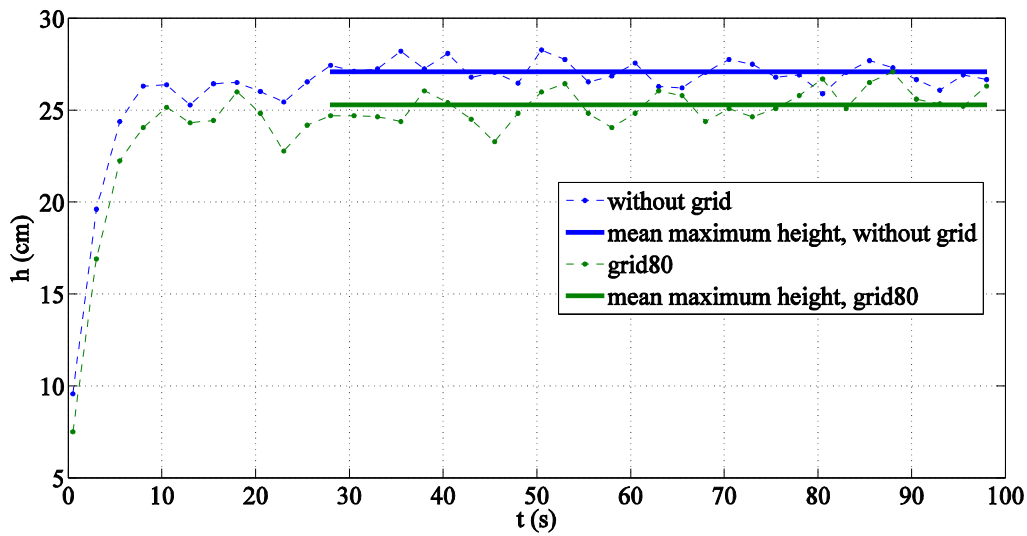


Figure 8: Maximum height reached by the jet as function of time

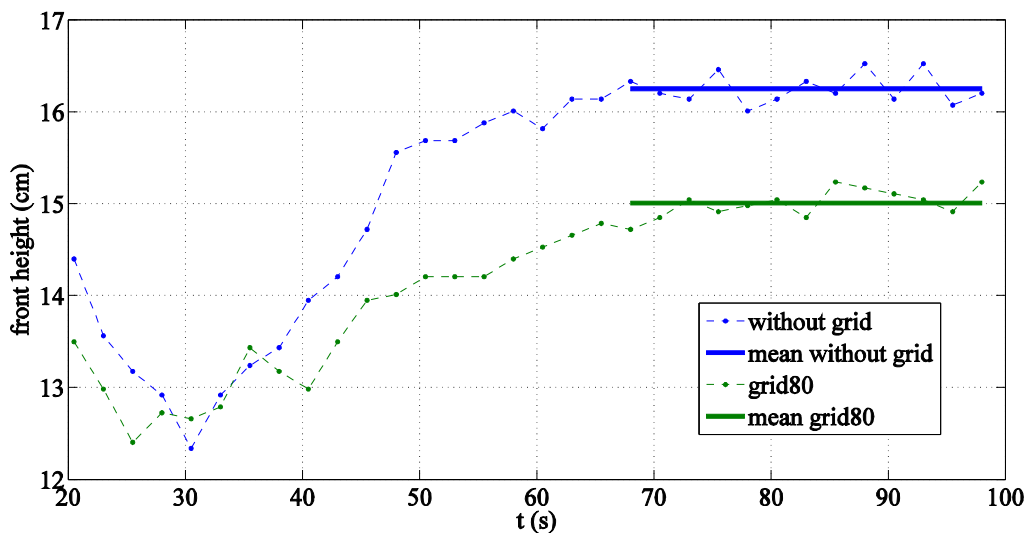


Figure 9: Intermediate height at which the spreading front develops

The power input required by the above-described SIS relates to the kinetic energy flux and, thus, to the third power of the reference velocity at injection point. Figures 8 and 9 suggest that a given spreading height may be reached using a lower momentum at injection point provided the turbulence intensity at the device outlet is reduced accordingly, resulting in a significant reduction in power input. A similar effect should be expected from a reduction of the swirl at the point of injection, an issue not addressed in this work.

Finally, the radial position of the spreading front as a function of time is illustrated in Figure 10. Since the flow rate was kept constant during all runs, the restricted and unrestricted flow configurations led to similar results.

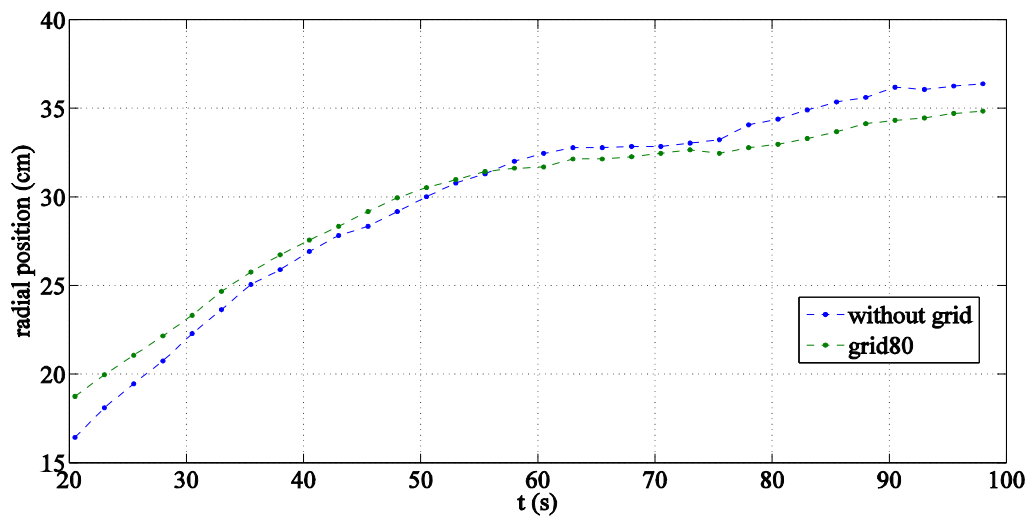


Figure 10: Spreading front radius as a function of time

5. Conclusion

Results here reported show that both the maximum height reached by a heavy-fluid jet as well as its spreading height decrease with increasing degree of turbulence at the point of injection. These results suggest that the generation of turbulence at the injection point may affect the efficiency of systems like the SIS. The inclusion of stationary or rotating blades or other mechanical device may lead to reduced jet turbulence, resulting in lower power requirements of the jetting machine without otherwise affecting the performance of an SIS.

References

- [1] Augsburger H K M 2000, Frost control in temperate climates through dissipation of cold air, *Aspects of Applied Biology* **61** 1
- [2] Guarga R, Mastrángelo P, Scaglione G and Supino E 2000, Evaluation of the SIS : a New Frost Protection Method Applied in a Citrus Orchard, Proceedings of the 9th. Congress of the Int. Soc. of Citriculture (Orlando, Florida). See also <http://www.frostprotection.com>.
- [3] Albertson M L, Dai Y B, Jensen R A and Rouse H 1950, Diffusion of a submerged jet, *Trans. A.S.C.E.* **115** 639-664
- [4] Baines W D, Turner J S and Campbell I H 1990, Turbulent fountains in an open chamber, *J. Fluid Mech* **212** 557-592
- [5] Bloomfield L J and Kerr R C 1998 Turbulent fountains in a stratified fluid, *J. Fluid Mech.* **358** 335-356
- [6] Bloomfield L J and Kerr R C 1999 Turbulent fountains in a confined stratified environment *J. Fluid Mech.* **389** 27-54
- [7] Baines P G 2002 Two dimensional plumes in stratified environments *J. Fluid Mech.* **471** 315-317
- [8] Baines P G 2005 Mixing regimes for the flow of dense fluid down slopes into stratified environments *J. Fluid Mech.* **538** 245-267
- [9] Ansong J K, Kyba P J and Sutherland B R 2008 Fountains Impinging upon a Density Interface *J. Fluid Mech.* **595** 115-139